14th IEA Heat Pump Conference
15-18 May 2023, Chicago, Illinois

Performance test of a gas-fired absorption heat pump with total recovery of exhaust heat applied for distributed space heating

Ding Lu[a], Zijian Liu[a,b] and Maoqiong Gong[a,b,*]

[a]Technical Institute of Physics and Chemistry, Chinese Academy of Sciences, Beijing 100190, China
[b]University of Chinese Academy of Sciences, Beijing 100049, China

Abstract

Under the background of carbon neutrality, efficient and low-carbon space heating in distributed areas away from the centralized network is a meaningful topic. In this paper, a gas-fired absorption heat pump was built and tested during winter in Langfang, a city near Beijing. The unit was driven by direct combustion of natural gas, and recovered low-grade heat from the ambient air. In order to increase the energy utilization ratio, solution preheating and intermediate evaporation was introduced. In order to enhance the internal heat recovery under low ambient temperatures, intermediate absorption was adopted. The measured performance showed that the outlet temperature of exhaust gas was lower than 35°C, indicating that both the sensible and latent heat were fully recovered. The average daily primary energy efficiency was over 1.58 and heating capacity was 30 kW, at the ambient temperature of -1.2°C, when supplying 45°C hot water for space heating. It was proven that the designed unit has great application potential in cold winter areas away from the centralized heating network.

Selection and/or peer-review under the responsibility of the organizers of the 14th IEA Heat Pump Conference 2023.

Keywords: absorption heat pump; performance analysis; natural gas; distributed heating; exhaust heat recoverytemperature

1. Introduction

Under the background of carbon neutrality, the reduction in fossil fuel usage and greenhouse gas emission are urgent and inevitable issues. Over 30% of the worldwide carbon emission is contributed by energy consumption in buildings [1]. Energy consumption for building space heating and cooling accounts for 58% and 41% in the urban and rural areas of China [2]. On the other hand, with the improvement of living standards and the advancement of urbanization in developing countries represented by China, the building area and energy consumption will be further increased [3]. Improving the space heating systems is of vital importance for energy conservation and carbon emission re-duction, and to some extent, is an important step towards achieving carbon neutrality.

In general, space heating can be realized by centralized networks in urban areas. Whereas, the huge initial capital cost for the network construction and the thermal losses along the pipe lines make centralized networks unaffordable in rural areas with low population density [4,5]. In terms of heating methods in areas away from the centralized networks, the wall-mounted gas furnace (GF) [6] and the compression heat pump (CHP) [7] are usually applied. The GF is low-efficient with primary energy efficiency (PEE) lower than 1. Even though the coefficient of performance (COP) of the electrically driven CHP can reach 3 [8], the PEE is still low since thermal power generation with 30-35% efficiency is the major way to generate electricity worldwide [9]. Even worse, these methods of separate heating greatly increase the initial investment of the consumers, and have more carbon emissions during production and operation.

As a result, the decentralized or house-central heating system for areas away from the centralized network has attracted wide attention. The absorption heat pump (AHP) can utilize different kinds of heat sources and provide heating with wide temperature range. For a single-stage system, its heating temperature ranges from

* Corresponding author. Tel.: +86-010-82543739; fax: +86-010-82543739.
E-mail address: gongmq@mail.ipc.ac.cn.

40°C to nearly 80°C, fitting for the heating demands of most occasions. It should be noted that the absorption system needs two kinds of heat sources: one is high-grade driving heat utilized in the generator, and the other is low-grade heat harvested in the evaporator. For a single-stage absorption system using LiBr-H2O or NH3-H2O as the working fluids, the generation temperature is in the range of 75-170°C [10], which can be easily achieved by natural gas combustion.

Compared with other systems including the GF and CHP, the AHP for district heating has the superiority of high PEE that can reach up to 1.3, due to the ability of utilizing additional low-grade heat through the evaporator. Zhang et al. [11] studied a hot water driven ground-source AHP for the district heating. They showed that the energy utilization efficiency was improved and the power consumption was reduced significantly, compared with those from the electrically-driven heat pump. Moreover, Wu et al. [12] studied a water-source AHP for the low temperature heating. The measured COP was 1.2 when the temperatures of the evaporator inlet, generator inlet and hot water outlet were set to -10°C, 130°C and 45°C, respectively. Moreover, the system could operate at the evaporator inlet temperatures of -18°C. Garrabrant et al. [13] studied a gas-fired NH_3-H_2O AHP, and the COP was 1.63 when producing 45 °C hot water under the ambient temperature of 20°C. Keinath et al. [14] investigated a gas-fired NH_3-H_2O AHP. The system achieved a COP of 1.74 when the ambient and water inlet temperatures were 20°C and 32°C, respectively.

The above-mentioned studies were all based on the single-effect system, which means the driving heat only triggered one generation process. Actually, the AHP systems were studied extensively aiming to find out the most suitable system con-figuration for the residential applications and district heating. Wu et al. [15] reviewed various heating methods based on the AHP technology, and discussed their application and development in different fields. Phillip et al. [16] investigated six different configurations, including double-effect, absorber augmented, double-effect regenerated, and generator-absorber heat exchange (GAX), and found that the optimal one is the GAX configuration. Kang et al. [17,18] studied the hybrid GAX system, where a compressor was added between the generator and the condenser to increase the heating temperature of the con-denser. Results showed that the absorber could provide 47°C hot water for district heating, and the condenser could provide hot water up to 100°C for other purposes. However, the GAX system was not suitable for cold regions, because as the ambient temperature decreases, the temperature overlaps between the generator and the absorber decreased or even disappeared. Garimella et al. [19] simulated a GAX system, and found that for the ambient temperature of 5.6°C, the COP reached up to 1.4, while when the ambient temperature de-creases to -30°C, the COP reduces sharply to 1.05. In order to improve the performance in cold regions, a double-stage [20] and a compression-assisted [21] AHP were developed.

In this paper, a gas-fired absorption heat pump was built and tested during winter in Langfang, a city near Beijing. The unit was driven by natural gas direct combustion, and recover low-grade heat from the ambient air. In order to increase the energy utilization ratio, solution preheating and intermediate evaporation was introduced. In order to enhance the internal heat recovery un-der low ambient temperatures, intermediate absorption was adopted.

2. System description

2.1. System Configuration

The schematic diagram of the gas-fired AHP system is shown in Figure 1. The system consists of four branches including the gas, water, solution and refrigerant branch, which are illustrated by the orange, blue, purple and green lines, respectively. Moreover, state points in the four branches are presented as G, W, S and R, separately. For example, W1 presents the return water state point, while G4 presents the flue gas outlet state point.

For the gas branch, the mixture of the natural gas and oxidizing air G1 enters the combustor, and the combustion heat is delivered to the generator. The high temperature flue gas G2 enters the solution preheater, heats the strong solution S1 flowing to the generator, and the temperature is reduced to a medium value. Then the medium temperature flue gas G3 enters the intermediate evaporator and the temperature is further reduced, and finally it is discharged to the ambient.

For the water branch, the return water W1 passes through the condenser, rectifier and absorber subsequently and absorbs the heat generated by each component. The water temperature increases gradually and the supply water W4 is supplied to hot consumers.

For the solution branch, the strong solution S1 is preheated by the flue gas, and after mixing with the reflux solution S0 from the rectifier, enters the generator and flows downward. The strong solution is first heated by

the generated weak solution S2, and generates part of the ammonia vapor. Then the solution is further heated by the gas combustion, and generates large amounts of ammonia vapor. In the meantime, mass transfer occurs between the solution and the vapor, along the packing. The generated weak solution S2 returns back to the generator to undergo the internal heat recovery process, hence its temperature decreases. After the expansion process, the weak solution S4 flows through the intermediate absorber and the absorber, and absorbs the ammonia vapor from the intermediate evaporator and the evaporator respectively. Finally, it turns to the strong solution S7, flowing to the solution tank. After pressurizing by the solution pump, the strong solution S8 enters the intermediate absorber to recover the absorption heat, and then it is further heated by the high temperature flue gas in the solution preheater.

For the refrigerant branch, the ammonia vapor R0 from the generator enters the rectifier. It is partially condensed to the reflux S0, while the remaining enters the condenser and is condensed to the liquid ammonia R2. After the subcooling and expansion process-es, the ammonia refrigerant enters the intermediate evaporator, recovers the waste heat of low temperature flue gas and is partially evaporated. The vapor-liquid mixture R5 enters the separator, where the vapor and liquid are separated. The vapor part R6 enters the intermediate absorber and is absorbed by the weak solution, while the liquid part R7 goes throttling and then enters the evaporator, where it absorbs heat from the ambient and is evaporated completely. After evaporation, the ammonia vapor R9 is superheated in the sub-cooler, and then enters the absorber and is absorbed by the solution.

Except for the above four branches, there exits another branch for defrosting, which is presented with the dotted purple lines in Figure 1. During the defrosting process, the de-frosting valve is opened and part of the intermediate solution S5 enters the evaporator directly, where it absorbs the ammonia refrigerant R8 and releases absorption heat for de-frosting. During this process, the system still operates, however the heating capacity is reduced. The larger the opening of the defrosting valve, the faster the defrosting speed, while the lower the heating capacity.

The main differences between the proposed system and the conventional system are shown in Fig. 2. The *P-T* diagrams were drawn under the basic working condition of -20℃ evaporation temperature and 180℃ generation temperature. The main innovation lies in the introduction of the intermediate evaporation and absorption processes. The ammonia condensate from the condenser was firstly throttled to intermediate pressure, and recovered waste heat from the flue gas. In this process, both the sensible and latent heat could be totally recovered by adjusting the intermediate pressure. Furthermore, the ammonia vapor, partially evaporated from the intermediate evaporator, entered the intermediate absorber, and the intermediate absorption heat was used to carry on internal heat recovery.

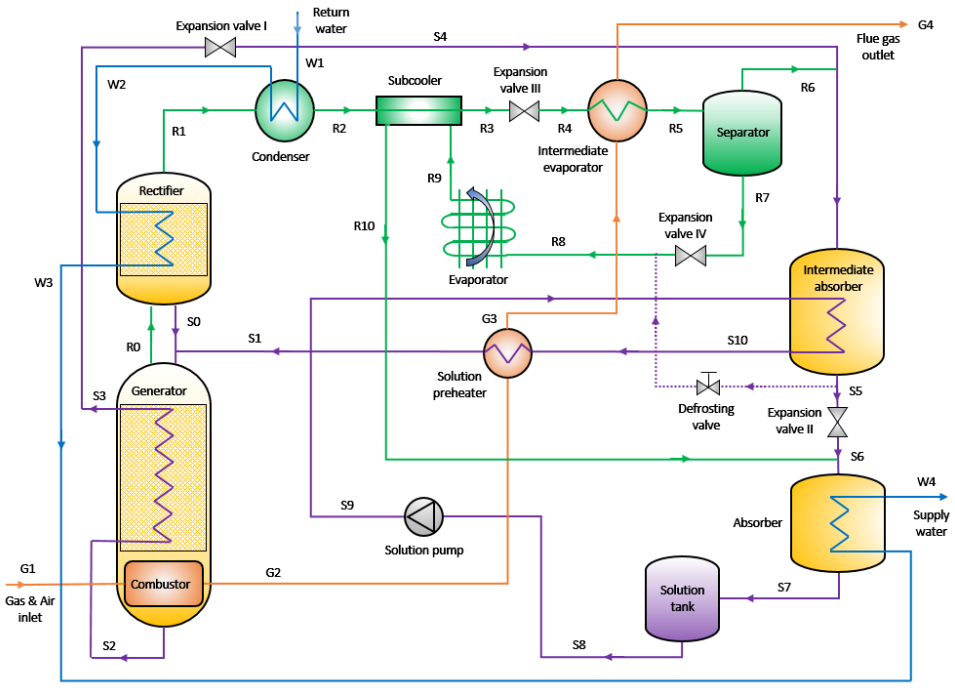

Fig. 1. Schematic diagram of the proposed gas-fired AHP system.

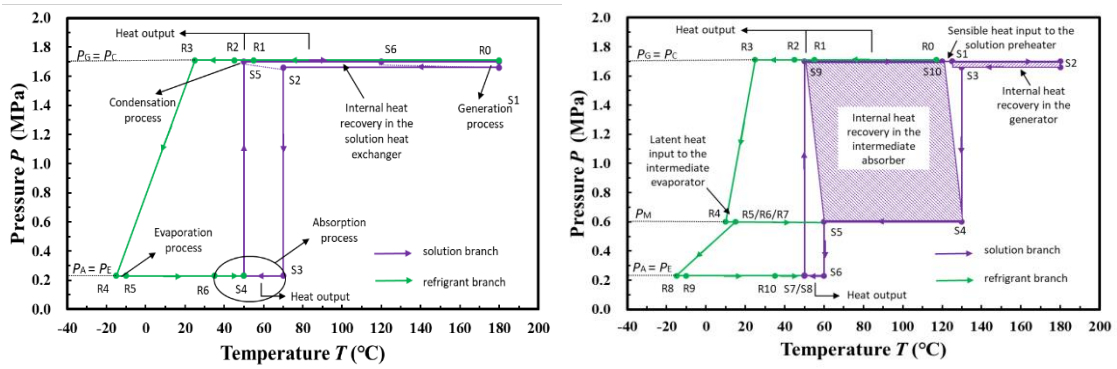

(a) (b)

Fig. 2. Comparison of *P-T* diagrams of the proposed system and the conventional one: (a) conventional system; (b) proposed system.

2.2. AHP unit

The 3D diagram and the photo of the gas-fired AHP unit with 30 kW heating capacity are shown in Figure 3. The unit had a compact design, with the dimension of 1360*1360*2260mm(L*W*H). The built AHP unit was expected to provide space heating for 3-4 families in the north of China in winter. Ammonia-water compare was used as the working fluid, considering that the system operated at low ambient temperatures. Natural gas was burned inside the unit as the driving heat source, and the evaporator could also harvest low-grade heat from the ambient air.

Fig. 3. 3D diagram and the picture of the gas-fired AHP unit.

Table 1. Details of the heat-exchange components of the gas-fired AHP unit.

Components	Types	Rated heat exchange Capacity (kW)
generator	falling film	20
rectifier	shell-and-tube	5
absorber	shell-and-tube	16
condenser	tube-in-tube	14
evaporator	plate-fin	11
intermediate absorber	tube-in-tube	18
intermediate evaporator	plate-fin	3
sub-cooler	tube-in-tube	1
solution preheater	plate-fin	1

Details of the heat-exchange components of the gas-fired AHP unit are shown in Table 1. The absorber was the shell-and-tube heat exchanger, while the condenser, sub-cooler and intermediate absorber adopted the tube-in-tube type. For the evaporator, intermediate evaporator and solution preheater, plate-fin heat exchangers were used. For the gas-fired generator, its structure is shown in Figure 4. Natural gas and air entered the combustion chamber at the bottom, where the natural gas was burned. The combustion heat was delivered to the ammonia-water solution through the solution jacket, which could also prevent the chamber wall from overheating. High-temperature flue gas from the combustion chamber raised through the gas pipeline, delivering heat to the solution flowing downward along the outer wall of the pipes. In order to enhance the heat and mass transfer insider the generator, the embossed threaded pipes and θ-ring packings were adopted.

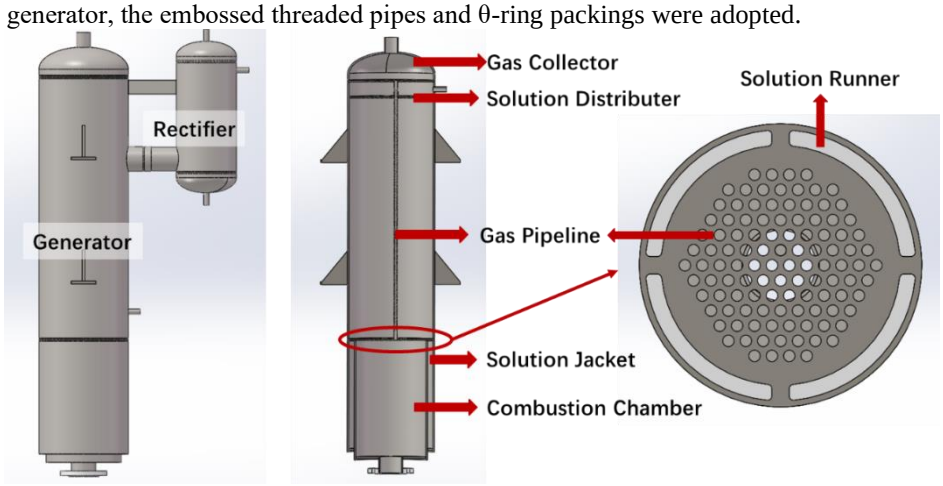

Fig. 4. Structure of the gas-fired generator.

3. Methods

Based on the AHP unit, system performance under typical heating conditions was investigated through the environmental tests in Langfang, a city near Beijing. The unit was designed in accordance with the worst operating conditions according to the preliminary simulation results, and all heat exchangers were designed in accordance with the maximum heat transfer capacity during the year-round operation. Therefore, the prototype could adapt to the change of working conditions with part-load operation in some conditions.

The AHP unit has more than 30 temperature measuring positions, 5 pressure measuring positions and 3 flowrate measuring positions, and the system operating conditions can be measured and recorded comprehensively. Details of the measuring components are shown in Table 2.

Table 2. Details of the measuring components of the gas-fired AHP unit.

Components	Type	Range	Accuracy
thermometers	PT100	-50~300°C	±0.25 °C
pressure meters	capacitance transmitter	0~2.5 MPa	±6.25 kPa
gas flowmeter	vortex	0~3 m^3/h	±0.045 m^3/h
water flowmeter	electromagnetic	0~6 m^3/h	±0.03 m^3/h
solution flowmeter	ultrasonic	0~2 m^3/h	±0.02 m^3/h
liquid level meter	floating ball	0~600 mm	±5mm

In the AHP unit, all the components that exchange heat with the surroundings adopted external medium countercurrent heat exchanger. The flowrate, inlet and outlet temperatures of the medium were measured to calculate the heat transfer capacity of each component, as are shown below [11]:

$$\text{driving heat} \quad Q_{\mathrm{D}} = V_{NG} \cdot q_{\mathrm{NG}} \tag{1}$$

$$\text{condensation heat} \quad Q_{\mathrm{C}} = m_{\mathrm{W}} \cdot c_{\mathrm{W}} \cdot \Delta T_{\mathrm{C}} = \rho_{\mathrm{W}} \cdot V_{\mathrm{W}} \cdot c_{\mathrm{W}} \cdot \left(T_{\mathrm{C,out}} - T_{\mathrm{C,in}}\right) \tag{2}$$

$$\text{rectification heat} \quad Q_{\mathrm{R}} = m_{\mathrm{W}} \cdot c_{\mathrm{W}} \cdot \Delta T_{\mathrm{R}} = \rho_{\mathrm{W}} \cdot V_{\mathrm{W}} \cdot c_{\mathrm{W}} \cdot \left(T_{\mathrm{R,out}} - T_{\mathrm{R,in}}\right) \tag{3}$$

$$\text{absorption heat} \quad Q_{\mathrm{A}} = m_{\mathrm{W}} \cdot c_{\mathrm{W}} \cdot \Delta T_{\mathrm{A}} = \rho_{\mathrm{W}} \cdot V_{\mathrm{W}} \cdot c_{\mathrm{W}} \cdot \left(T_{\mathrm{A,out}} - T_{\mathrm{A,in}}\right) \tag{4}$$

where V_{NG} and q_{NG} are the volume flow rate and calorific value of standard volume of the natural gas; m_W, V_W, and c_W are the mass flowrate, volume flow rate, density and specific heat of the water; ΔT , T_{in} and T_{out} are the temperature difference, inlet temperature and outlet temperature of each component. The total heating capacity of the AHP unit is the sum of the heat from the condenser, rectifier and absorber:

$$\text{total heating capacity} \quad Q_H = Q_C + Q_R + Q_A \tag{5}$$

The heating performance of the AHP unit is presented by the primary energy efficiency PEE, which is the ratio of the heating capacity to the driving heat (i.e., the calorific value of the consumed natural gas):

$$\text{primary energy efficiency} \quad \text{PEE} = \frac{Q_H}{Q_D + W/\eta} \tag{6}$$

where W is the total power consumption of the AHP unit, and η is the power generation efficiency in China, which is about 35% [9].

4. Results and Discussion

4.1. Start-up performance

The startup sequence of the AHP unit followed this order: firstly, the gas combustor started, then the refrigerant valve opened, and finally the water chiller started. The refrigerant valve was closed at first, in order to quickly reach the required generation temperature and pressure. Fig. 5 shows the startup performance of the gas-fired AHP unit. It should be noted that a test run was conducted the day before, and the solution temperature in the generator reduced to about 100°C after overnight cooling.

It is found that a rapid growth in the generation temperature and pressure happened after starting the gas combustor, and the generation pressure reached up to 1.6 MPa within 7 minutes. Meanwhile the refrigerant valve opened, and the generation pressure reduced to 1.2 MPa, while the intermediate pressure raised immediately to 0.8 MPa. It should also be noted that the outlet temperature of flue gas reduced to 37°C after the intermediate evaporation process got involved.

When the solution temperature and pressure reached 90% of the target values, the water chiller started. The generated ammonia vapor was condensed in the rectifier, and then flowed into the solution. This process caused reduction in the solution temperature and pressure at first, and then tended to be stationary. 50 minutes after starting up, the supply water temperature reached the stable value of 43°C, and the AHP unit Began normal operation.

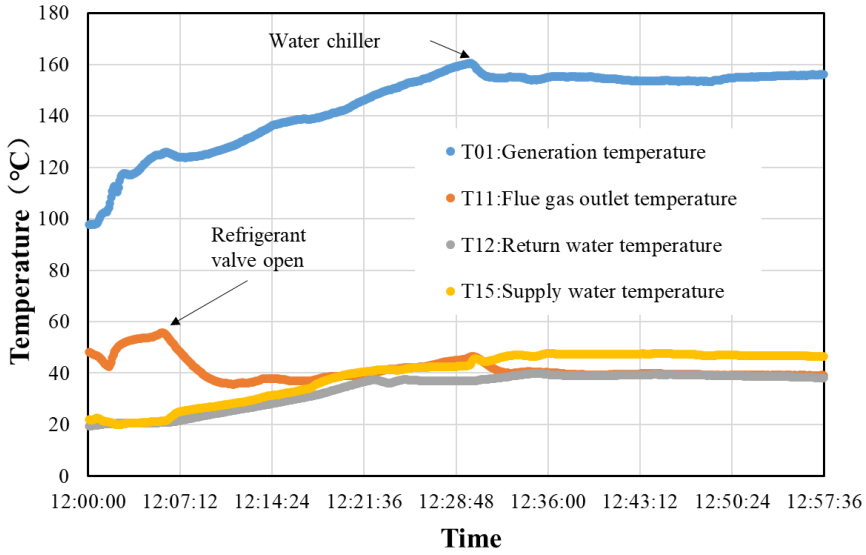

(a)

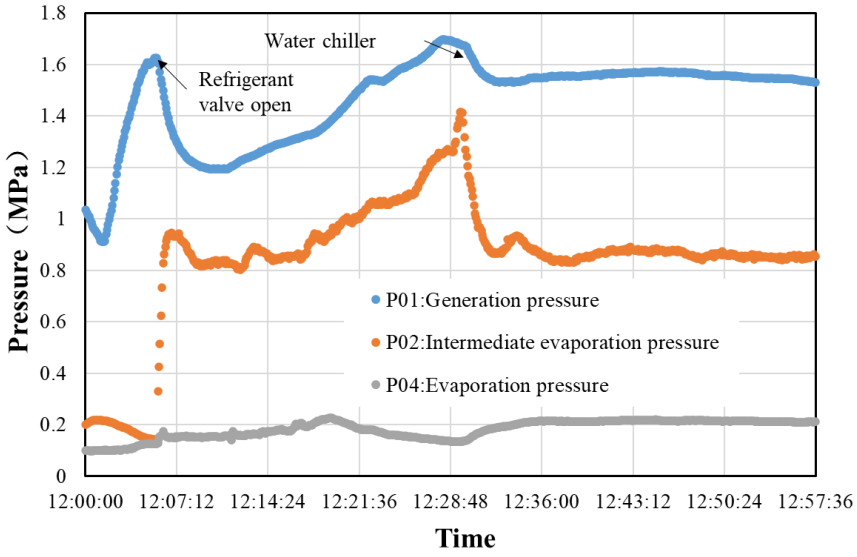

(b)

Fig. 5. Start-up performance of the gas-fired AHP unit: (a) Key temperature parameters variation; (b) Key pressure parameters variation.

4.2. Performance under basic working condition

The performance of the gas-fired AHP unit was analyzed in detail under the basic working condition: the evaporation temperature was -1.2°C, the return water temperature was 37.0°C, and the supply water temperature was 45.2°C. Detailed data of key parameters are shown in Table 3. The return water of 37.0°C passed in sequence through the condenser, rectifier and absorber, and its temperature increased to 40.2, 41.3 and 45.1°C, respectively, with flow rate keeping at 3.26 m3/h. It is shown that by introducing the intermediate process, the outlet temperature of flue gas was reduced to 38.6°C, which was lower than its dew point, indicating that the gas-fired AHP unit had ability to fully recover both the sensible and latent heat. It is also shown in Table 3 that the system high pressure, intermediate pressure and low pressure were 1.6 MPa, 0.8-0.9 MPa and 0.2-0.3 MPa, respectively. Moreover, the intermediate absorption pressure was 60 kPa lower than the intermediate evaporation pressure, and the absorption pressure was 70 kPa lower than the evaporation pressure, due to the flow resistance and the obstruction of check valves.

Table 3. Data of key parameters under the basic working condition.

Parameters	Value
ambient temperature	-1.2°C
evaporation temperature	-7.5°C
generation temperature	156.2°C
return water temperature	37.0°C
condenser outlet water temperature	40.2°C
rectifier outlet water temperature	41.3°C
supply water temperature	45.1°C
generator outlet gas temperature	117.0°C
Outlet temperature of flue gas	38.6°C
generation pressure	1.62 MPa
intermediate evaporation pressure	0.93 MPa
intermediate absorption pressure	0.87 MPa
evaporation pressure	0.29 MPa
absorption pressure	0.22 MPa
natural gas volume flowrate	1.82 Nm^3/h

water volume flowrate	3.26 m^3/h
power consumption	0.52 kW

Based on the measured data, the heat duty or power consumption of the main component, as well as the performance of the AHP unit are shown in Table 4. When the ambient temperature was -1.2°C, the AHP unit could provide 30.8 kW heating capacity to heat the water from 37 to 45°C, and the PEE was 1.58.

Table 4. Performance of the gas-fired AHP unit.

Parameters	Value
ambient temperature	-1.2°C
supply/return water temperature	45/37°C
condensation heat	12.2 kW
rectification heat	4.2 kW
absorption heat	14.5 kW
heating capacity	30.8 kW
calorific of natural gas	18.0 kW
power consumption	0.52 kW
primary energy efficiency PEE	1.58

4.3. Influence of the ambient temperature

Figure 5 shows the influence of the ambient temperature on the system performance. It is indicated that as the ambient temperature reduced from 7.2°C to -7.8°C, the primary energy efficiency reduced from 1.82 to 1.38. At the lower ambient temperature, the ammonia evaporation was impeded, and the opening of the electronic expansion valve decreased. As a result, the recovered low-grade ambient heat and the PEE of the AHP unit reduced.

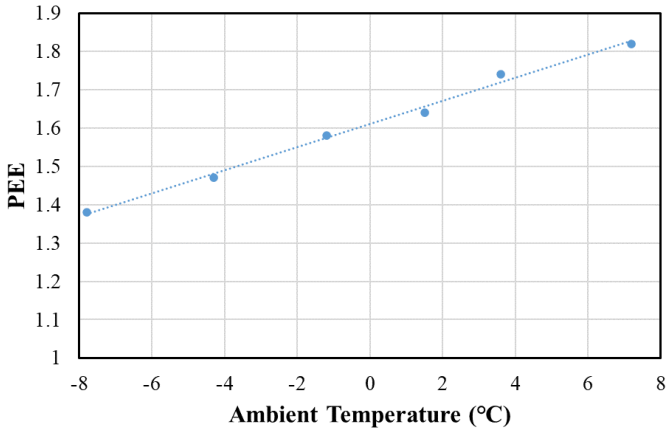

Fig. 5. Influence of the ambient temperature on the system performance.

5. Conclusions

In this paper, a gas-fired absorption heat pump was built and tested during winter in Langfang, a city near Beijing. The unit was driven by natural gas direct combustion, and recovered low-grade heat from the ambient air. In order to increase the energy utilization ratio, solution preheating and intermediate evaporation was introduced. In order to enhance the internal heat recovery under low ambient temperatures, intermediate absorption was adopted.

1. The measured performance showed that the exhaust gas outlet temperature was lower than 35°C, indicating that both the sensible and latent heat were fully recovered.

2. The average daily primary energy efficiency was over 1.58 and heating capacity was 30 kW, at the ambient temperature of -1.2°C, when supplying 45°C hot water for space heating.

It was proven that the designed unit has great application potential in cold winter areas away from the centralized heating network.

Acknowledgements

The authors would like to thank the support of the National Natural Sciences Foundation of China (No. 52206033).

References

[1] Kingma B, Lichtenbelt WV. Energy consumption in buildings and female thermal demand. Nat Clim Chang. 2015;5(12): 1054-1056.
[2] Zheng X, Wei C, Qin P, Guo J, Yu Y, Song F, et al. Characteristics of residential energy consumption in China: Findings from a household survey. Energy Policy. 2014;75:126-35.
[3] Center TUBESR. Annual Report on China Building Energy Efficiency: China Architecture and Building Press; 2020.
[4] Buffa S, Cozzini M, D'Antoni M, Baratieri M, Fedrizzi R. 5th generation district heating and cooling systems: A review of ex-isting cases in Europe. Renew Sust Energ Rev. 2019;104:504-22.
[5] Lake A, Rezaie B, Beyerlein S. Review of district heating and cooling systems for a sustainable future. Renew Sust Energ Rev. 2017;67:417-25.
[6] Zhang QL, Hao YY, Sun DH, Nie Q, Jin LW. Research on the Clean Energy Heating Systems in Rural Beijing. Joint Conference of the World Engineers Summit / Applied Energy Symposium and Forum - Low Carbon Cities and Urban Energy (WES-CUE). Singapore, SINGAPORE: Elsevier Science Bv; 2017. p. 137-43.
[7] Wu D, Hu B, Wang RZ. Vapor compression heat pumps with pure Low-GWP refrigerants. Renew Sust Energ Rev. 2021;138: 110571.
[8] Fumo N, Chamra LM. Analysis of combined cooling, heating, and power systems based on source primary energy con-sumption. Applied Energy. 2010;87:2023-30.
[9] Zoungrana A, Çakmakci M. From non‐renewable energy to renewable by harvesting salinity gradient power by reverse elec-trodialysis: A review. International Journal of Energy Research. 2020;45:3495-522.
[10] Florides GA, Kalogirou SA, Tassou SA, Wrobel LC. Design and construction of a LiBr-water absorption machine. Energy Conv Manag. 2003;44:2483-508.
[11] Qunli Z, Mingkai C, Qiuyue Z, et al. Research on a new district heating method combined with hot water driven ground source AHP. Energy Procedia 2015; 75: 1242-1248.
[12] Wu W, Ran S, Shi W, et al. NH3-H2O water source AHP (WSAHP) for low temperature heating: Experimental investigation on the off-design performance. Energy 2016; 115: 697-710.
[13] Garrabrant M, Stout R, Glanville P, Fitzgerald J, Keinath C. Development and validation of a gas-fired residential heat pump water heater-final report (No.DOE/EE0003985-1). Stone Mountain Technologies, Inc; 2013.
[14] Keinath C M, Garimella S, Garrabrant M A. Modeling of an ammonia–water AHP water heater for residential applications. International Journal of Refrigeration 2017; 83: 39-50.
[15] Wu W, Wang B, Shi W, et al. Absorption heating technologies: a review and perspective. Applied Energy 2014; 130: 51-71.
[16] Phillips B A. Development of a high-efficiency, gas-fired, AHP for residential and small-commercial applications. NASA STI/Recon Technical Report N, 1990, 91.
[17] Kang Y T, Kashiwagi T. An environmentally friendly GAX cycle for panel heating: PGAX cycle. International Journal of Refrigeration 2000; 23(5): 378-87.
[18] Kang Y T, Hong H, Park K S. Performance analysis of advanced hybrid GAX cycles: HGAX. International Journal of Refrig-eration 2004; 27(4): 442-8.
[19] Garimella S, Christensen R N, Lacy D. Performance evaluation of a generator-absorber heat-exchange heat pump. Applied Thermal Engineering 1996; 16(7): 591-604.
[20] Wu W, Zhang XL, Li XT, Shi WX, Wang BL. Comparisons of different working pairs and cycles on the performance of ab-sorption heat pump for heating and domestic hot water in cold regions. Applied Thermal Engineering 2012; 48:349–58.
[21] Wu W, Shi W, Wang B, et al. A new heating system based on coupled air source absorption heat pump for cold regions: Energy saving analysis. Energy Conversion and Management 2013; 76: 811-817.
[22] Lu D, Bai Y, Zhao Y, Dong X, Gong M, Luo E, et al. Experimental investigations of an absorption heat pump prototype with intermediate process for residential district heating. Energy Conversion and Management. 2020;204:112323.